CTAP-Minimized Scheduling Algorithm for Millimeter-Wave-Based Wireless Personal Area Networks

Hsi-Lu Chao, *Member, IEEE*, and Ming-Pei Hsu

***Abstract*—Beamforming is used in IEEE 802.15.3c networks to avoid high propagation attenuation and path loss and improve the overall system throughput by exploiting spatial channel reuse. In this paper, we introduce design challenges of scheduling in beamforming-enabled IEEE 802.15.3c networks. These challenges include positioning, axis alignment, and interference relation verification. We then propose a joint design of axis alignment, positioning, and scheduling. The objectives of the proposed joint design are to reduce the consumed channel time, increase the degree of spatial channel reuse, and improve the channel utilization. For positioning, we define and prove a sufficient condition for anchor selection to improve positioning accuracy. The designed channel time allocation period (CTAP)-minimized scheduling algorithm is depicted as a two-layer flow graph, and it consists of the following three phases: 1) layer-1 edge construction; 2) layer-2 edge construction; and 3) scheduling. Through the observation of transmission and reception beams, we define a rule to verify the interference relation of two flows. In addition, given correct topology information, we prove that CTAP-minimized uses the least time to serve all data flows. We evaluate and compare our algorithm with existing approaches through simulations. The observed performance metrics include utilized channel time, system throughput, scheduling efficiency, and spatial channel reuse degree. The results show that CTAP-minimized performs well and achieves its objectives.**

***Index Terms*—Axis alignment, beamforming, IEEE 802.15.3c, positioning, scheduling.**

I. Introduction

MILLIMETER-WAVE wireless personal area networks (mmWave WPANs) that operate in the 60-GHz band have recently attracted much attention due to their high-data-rate transmission capability (more than 3 Gb/s) such that numerous high-bandwidth-demand indoor wireless applications become possible. Examples of such applications include uncompressed transmission of high-definition television (HDTV), high-speed Internet access, and wireless gigabit Ethernet. Existing wireless local area networks (WLANs) and wireless personal area networks (WPANs) cannot support these applications, because the required data rate is far beyond their capabilities. As a result, mmWave WPAN has become a major trend in short-range communication systems, leading to active research and standardization efforts in this area, e.g., IEEE 802.15.3c [1].

An IEEE 802.15.3c network is called a piconet, which is formed in ad hoc fashion. Among a group of devices (DEVs), one of these DEVs is designated as the piconet coordinator (PNC). The PNC is responsible for providing synchronization and management for the piconet. In addition, the PNC manages the access control of the remaining DEVs. The necessary control information is embedded in beacon messages. Upon receiving a beacon message, DEVs are aware of the existence of the PNC, and they learn when and how to access the channel. The channel time is divided into a sequence of superframes, and each superframe consists of the following three portions: 1) beacon; 2) contention access period (CAP); and 3) channel time allocation period (CTAP). Each superframe starts with a beacon, followed by a CAP. The channel access of the CAP is governed by the carrier-sense multiple access/collision avoidance (CSMA/CA) method. The remaining time in a superframe is the CTAP, which provides time-division multiple access (TDMA)-type of communications. The CTAP comprises one management channel time allocation (MCTA) and multiple channel time allocations (CTAs). MCTA is for DEVs to issue their transmission requests to the PNC, whereas CTAs are for DEVs to transmit data frames.

A. Problem Description

In IEEE 802.15.3c piconets, beamforming is used to avoid significant path loss, increase the antenna gain, and extend the transmission range. With beamforming, DEVs can only transmit and receive signals at a specific direction. This approach means that exploiting spatial channel reuse among data flows can improve the scheduling efficiency and channel utilization. However, in the scheduling algorithm defined in the IEEE 802.15.3 standard (herein called *conventional scheduling*), each CTA is allocated to only one data flow. Thus, conventional scheduling does not get benefits from beamforming to improve the overall system throughput.

In this paper, we study the CTA problem by exploiting beamforming characteristics. It is essential for a pair of DEVs to properly set their antenna array when implementing

Manuscript received July 9, 2010; revised January 24, 2011 and May 26, 2011; accepted May 31, 2011. Date of publication July 7, 2011; date of current version October 20, 2011. This work was supported in part by the National Chiao Tung University/MediaTek Joint Research Center under Grant 99Q583. The review of this paper was coordinated by Prof. H. Hassanein.

H.-L. Chao is with the Department of Computer and Information Science, National Chiao Tung University, Hsinchu 300, Taiwan (e-mail: hlchao@cs.nctu.edu.tw).

M.-P. Hsu was with the National Chiao Tung University, Hsinchu 300, Taiwan. She is now with the Software Eng'g Div I, Wireless Communications Business Unit, MediaTek Inc., Taipei 114, Taiwan (e-mail: mingpei.hsu@gmail.com).

Color versions of one or more of the figures in this paper are available online at http://ieeexplore.ieee.org.

Digital Object Identifier 10.1109/TVT.2011.2161354

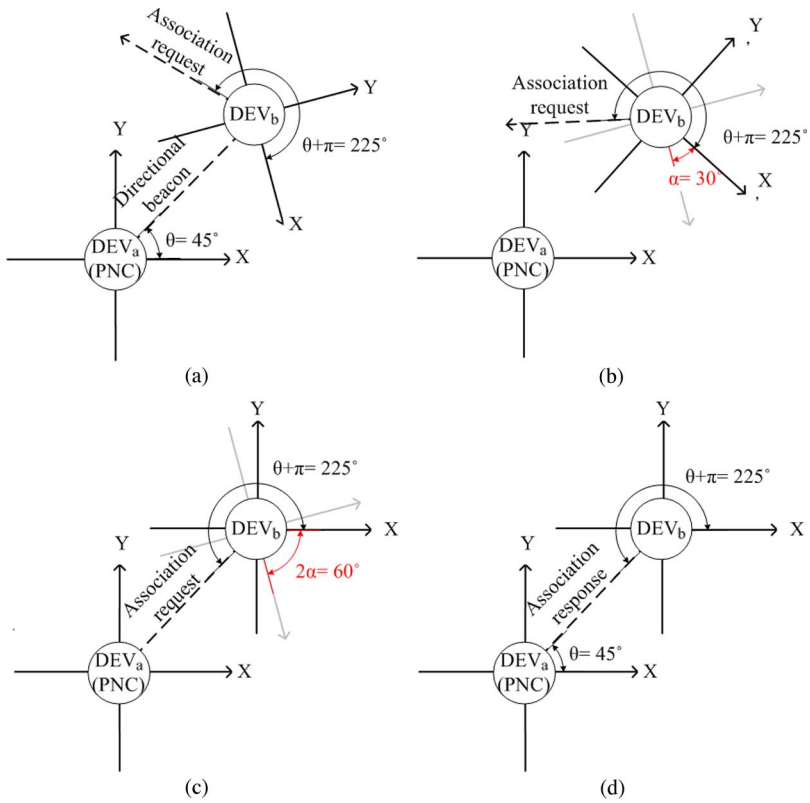

Fig. 1. Axis alignment. (a) DEV_b listens to beacons sent from the PNC. (b) DEV_b sends an association request to the PNC. (c) DEV_b rotates its axes and resends an association request to the PNC. (d) PNC replies the association request to DEV_b.

beamforming [2]–[4]. To achieve this condition, a pair of DEVs must know each other's position. Due to being responsible for CTA, a PNC must know the interference relation of DEVs to schedule noninterfered flows in a CTA. Positioning is an approach for a PNC to collect DEVs' interference relation. Among existing positioning work, signal-measurement-based approach is not suitable for mmWave networks because of serious signal fading. Furthermore, one common assumption of existing work [5]–[7] is the predeployment of self-positioning-capable anchors. Through these anchors, other nodes then determine their coordinates. However, where we can deploy anchors should first be tackled. The reason is that a piconet is dynamically formed and predeployed anchors cannot work well when encountering obstacles (e.g., walls and furniture).

Both positioning and axis consistency affect multimedia content delivery. When the axis system is not consistent in a piconet, a PNC may schedule interfered flows in a CTA, and thus, a collision occurs. Moreover, the data transmission of a pair of DEVs may fail. Fig. 1(a) illustrates the significance of axis consistency. When DEV_b receives beacon messages that are sent by the PNC (i.e., DEV_a in this example), it knows that it is located in the first quadrant of the PNC and the PNC is in its third quadrant. In such a situation, transmission from DEV_b to the PNC (and *vice versa*) always fails due to the problem of axis inconsistency.

Although axis alignment and positioning are crucial for beamforming-enabled 802.15.3c networks, both factors are not within the scope of the standard. In this paper, we design a scheduling mechanism for beamforming-enabled mmWAVE networks. To exploit the maximum degree of spatial channel reuse and achieve the maximum channel utilization, the designed scheduling mechanism integrates with both axis alignment and positioning.

B. Related Work

Recent research issues for IEEE 802.15.3c networks include hardware implementation and system architecture design for 60-GHz systems, beamforming protocol design, performance analysis and interference estimation, and resource management [8]–[22]. The focus of this paper is resource management, particularly on channel time scheduling.

In the scheduling algorithm defined in the IEEE 802.15.3 standard (*conventional scheduling*), each CTA is allocated to only one data flow. Thus, conventional scheduling does not get benefits from beamforming to improve the overall system throughput. In [18], an interference-avoiding scheduling is proposed. A handler is responsible for discovering concurrent transmission-capable flows by ensuring that the accumulated interference is less than a predefined threshold. Every time a data flow is added to calculate the induced interference, the handler examines all flow combinations to discover the optimal scheduling result.

In [19], the following two types of communications are considered: 1) direct paths and 2) relay paths. To improve the overall system throughput, a single-hop flow will be served through a relay path if this relay path can share CTAs with some direct paths. The condition of sharing CTAs is an acceptable

signal-to-noise-plus-interference ratio (SINR) that is measured at receivers. Similar to [18] for interference ratio measurement, in virtual time-slot allocation (VTSA) [20], a PNC preconstructs a cochannel interference table for all DEVs. Every time the PNC receives a new channel time request, it allocates this new flow to the CTA, where the cochannel interference value among all values is the least.

In [21], the author proposed a scheduling approach called the randomized exclusive-region-based scheduling (REX) scheme. The main idea is that the receiver of a specific flow has an exclusive region (ER) and that the senders of other flows should be located outside the ER to ensure noninterference. DEVs can be equipped with either omnidirectional or directional antennas, and thus, REX defines four kinds of ERs. The ER condition is that exactly one sender is located inside the ER of a receiver. Multiple flows are allowed to be scheduled in the same CTA only if they satisfy the ER condition. In REX, one flow is selected to be allocated a time slot; then, all remaining flows are verified based on the ER condition to discover spatial channel-reuse-capable flows.

In [22], directional transmission scheduling (DTS) is proposed. In DTS, each DEV maintains a neighbor profile, in which the IDs and directions of one-hop neighbors are recorded. When a DEV has data to send, it issues a transmission request with its own neighbor profile to the PNC. The PNC performs scheduling based on the received transmission requests and the corresponding neighbor profiles. To avoid interference, for a specific data flow, DEVs that are located in the sender's neighboring sectors are forbidden to simultaneously send data. For example, if the intended receiver is located in its potential sender's sector 3, the neighbor profile of this flow is sectors 2–4. Other senders are forbidden to send data to the directions of sectors 2–4.

In short, the adopted criteria for exploiting the advantage of the beamforming technology in existing scheduling mechanisms include the SINR value [18]–[21] and location profile [22]. The former parameter explores flows that satisfy the condition of spatial channel reuse through pairwise interactive interference measurement. Thus, these approaches maintain a large database for storing the interference information. Moreover, the distance between a sender and a receiver is one key parameter for SINR estimation in some propagation models. However, most of the existing works do not describe the utilized positioning scheme; instead, they assumed that the coordinates of DEVs are known. Location-profile-based scheduling has to record not only the desired reception sector but its adjacent sectors to avoid interference as well. Thus, it restricts the throughput improvement due to the lack of more accurate topology information, and the PNC has to maintain all DEVs' neighbor profiles.

C. Contributions

A scheduling mechanism with axis alignment and anchor selection has not been studied for IEEE 802.15.3c networks. In this paper, we design a joint algorithm of axis alignment, positioning, and scheduling for IEEE 802.15.3c networks. To the best of our knowledge, this paper is the very first work that jointly considers these three factors for IEEE 802.15.3c networks. The contributions of our approach are summarized as follows.

1) Unlike existing positioning work, our algorithm can be applied to one random-topology environment without preconfigured anchor nodes.
2) We define and prove a sufficient condition for anchor selection, which is one of the key conditions to improve positioning accuracy.
3) By taking transmission and reception beam patterns into account, the proposed verification rules of concurrent transmission most exert the advantage of beamforming.
4) We prove that the designed scheduling algorithm uses the least channel time to accommodate all data flows' time requirements.

The rest of this paper is organized as follows. Section II describes the axis alignment and positioning. Section III introduces the CTAP-minimized scheduling algorithm. Section IV presents and discusses the performance evaluation. This paper is concluded in Section V.

II. Axis Alignment and Positioning

As described in Section I, axis alignment and positioning are two important schemes to improve scheduling efficiency. Unlike some existing positioning approaches, our mechanism does not deploy landmarks or pre-configurable anchors in advance. In this section, we first briefly describe some preliminaries, and then the operations of axis alignment and positioning.

A. Preliminary

Piconets are dynamically formed, and DEVs can freely join and leave a piconet. A PNC announces its existence through periodically broadcasting beacons in each direction. When a DEV is activated, it first scans all channels to discover the existence of a PNC. When receiving beacon messages, the DEV exchanges an association request/response with the PNC to join the piconet, and then, it becomes one member; otherwise, it initiates a piconet and serves as a PNC. PNCs and DEVs are equipped with configurable beamforming antennas, and thus, they transmit or receive data frames at a certain direction at a time.

A PNC embeds the information of transmission beamwidth φ_t and transmission azimuth angle θ_t in beacons. Here, the *transmission beamwidth* and *transmission azimuth angle* represent the covered angle of the transmission beam pattern and the angle between the direction of the transmission beam and the x-axis in the azimuth plane, respectively.

The statistical model proposed in [23] is adopted for describing general properties of 60-GHz indoor channels and estimating the propagation distance between a transmitter and a receiver. In [23], the path loss from a transmitter to a receiver is determined by taking

$$\overline{PL}(d)_{[dB]} = P_{t[dBm]} + G_{t[dB]} + G_{r[dB]} - P_{r[dBm]} \quad (1)$$

where $PL(d)$ is the measured path loss over distance d (in meters), P_t and P_r are the transmitter and receiver powers,

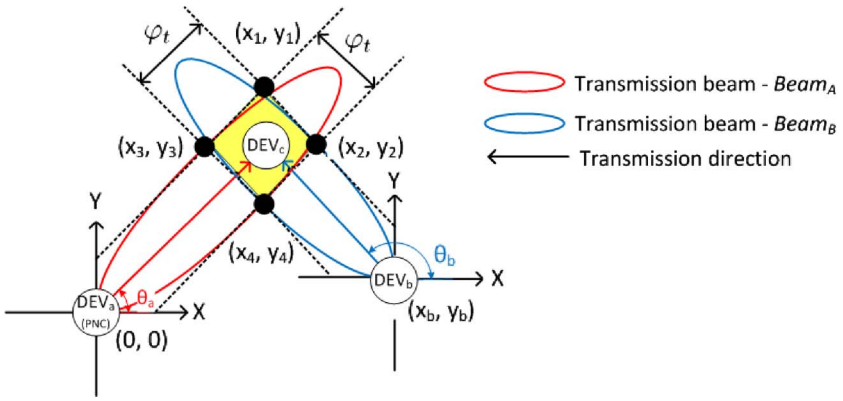

Fig. 2. Example that shows an IR.

respectively, and G_t and G_r are the antenna gains of the transmitter and the receiver, respectively. In addition, $PL(d)$ can be described by the path-loss exponent model as follows:

$$\overline{PL}(d) = 10\log_{10}\left(\frac{4\pi d_0}{\lambda}\right)^2 + 10n\log_{10}\left(\frac{d}{d_0}\right) \quad (2)$$

where λ is the wavelength, n is the path-loss exponent, and d_0 is a reference distance. Note that the first term is exactly the free-space path loss. In [24], the recommended setting of d_0 is 1 m. The path-loss exponent characterizes how fast the path lost increases with the increase of the transmitter–receiver separation, and its setting depends on the propagation environment, e.g., line-of-sight (LOS) or non-line-of-sight (NLOS) transmission, office, or corridor environments. In this paper, we assume that the received signal power is mainly from the LOS path. Based on the experiment results shown in [23], the n value is set to be 2.

B. Axis Alignment

Axis alignment is executed when a DEV joins in a piconet. When a newly joined DEV receives a beacon of θ_t transmission azimuth angle, it replies an association request to the PNC. If $0 \leqq \theta_t \leqq \pi$ (i.e., the DEV is located in the first or second quadrant of the PNC), the DEV sets its transmission azimuth angle as $(\theta_t + \pi)$; otherwise, the DEV is located in the third or fourth quadrant of the PNC, and its transmission azimuth angle is $(\theta_t - \pi)$. If this newly joining DEV does not receive an association reply sent by the PNC, it counterclockwise rotates its x- and y-axes with α° and resends the association request. Here, α is a predefined constant (in degrees). This axis rotation repeats until the DEV has received an association reply. Therefore, the axes of all DEVs are aligned with the PNC.

One example is shown in Fig. 1. In this example, DEV_a is the PNC, and DEV_b is a newly joining DEV. α is 30° in this example. The transmission azimuth angle carried in a beacon is 45°. Because $0 \leqq \theta_t \leqq \pi$, upon receiving the beacon, DEV_b responds with an association request to DEV_a by setting the transmission azimuth angle to be 225° [see Fig. 1(a)]. If DEV_b does not receive the corresponding association reply, it counterclockwise rotates its x- and y-axes with 30° and resends the association request [see Fig. 1(b)]. After the second axis rotation, DEV_b receives the corresponding association reply [see Fig. 1(c) and (d)].

C. Positioning

After performing axis alignment, a PNC realizes the quadrants in which DEVs are located. Instead of PNC relaying, data are directly delivered among DEVs. In such a case, the PNC cannot derive the interference relation of data flows only through the quadrant information. Positioning is an approach to provide a PNC the interference relation among all flows to decrease transmission collision and increase network throughput. In this paper, positioning is the process for nodes to self determine their coordinates.

First, because a piconet is initiated by a PNC, the coordinate of this PNC is (0, 0). Then, the coordinate of the second joining DEV is estimated by the following two parameters: 1) the transmission azimuth angle θ_t and 2) the propagation distance d. The propagation distance is estimated through the propagation mode. Indeed, upon knowing P_t, P_r, G_t, and G_r, we can derive $PL(d)$ by using (1). Further substituting $PL(d)$, d_0, λ, and n into (2), we can derive the estimated propagation distance d. Therefore, the estimated coordinate of the second joining DEV is $(d\cos\theta_t, d\sin\theta_t)$.

For the remaining joining DEVs, they can calculate their coordinates by selecting at least a pair of anchors. A DEV can be an anchor when its coordinate is known. To improve positioning accuracy, the PNC is always the first anchor of an anchor pair. The problem now is how we can properly select the second anchor. We first give one definition and then explore the sufficient condition of anchor selection as follows.

Definition 1: The intersection region (IR) is the overlapped area of two transmission beams. In Fig. 2, the area colored yellow is the IR of $Beam_A$ and $Beam_B$.

Proposition 1: For a DEV to be positioned, let S be the set of all second-anchor candidates. The transmission azimuth angles of the PNC and anchor candidate DEV_i are denoted by θ_a and θ_i, respectively, where $DEV_i \in S$. If $j = \arg\min((\pi/2) - |\theta_a - \theta_i|)\ \forall i$, then among all candidates, (PNC, DEV_j) is the best anchor pair.

Proof: For simplicity and without loss of generality, we use Fig. 2 to illustrate our proof. In Fig. 2, we assume that two anchors of DEV_c are DEV_a, i.e., the PNC and whose

coordinate is (0, 0), and DEV_b, whose coordinate is (x_b, y_b). In addition, their transmission azimuth angles are θ_a and θ_b, respectively. The width of the transmission beam pattern is φ_t. The maximum positioning error of the actual and the estimated coordinates may occur at one of the four vertices of the IR. We denote the coordinates of the four vertices as (x_1, y_1), (x_2, y_2), (x_3, y_3), and (x_4, y_4). The coordinates of four vertices are listed as follows:

$$\begin{cases} x_1 = \frac{y_b-(\tan\theta_b)x_b+(\sec\theta_b-\sec\theta_a)\frac{\varphi_t}{2}}{\tan\theta_a-\tan\theta_b} \\ y_1 = (\tan\theta_a)x_1 + (\sec\theta_a)\frac{\varphi_t}{2} \end{cases} \tag{3}$$

$$\begin{cases} x_2 = \frac{y_b-(\tan\theta_b)x_b+(\sec\theta_b+\sec\theta_a)\frac{\varphi_t}{2}}{\tan\theta_a-\tan\theta_b} \\ y_2 = (\tan\theta_a)x_2 - (\sec\theta_a)\frac{\varphi_t}{2} \end{cases} \tag{4}$$

$$\begin{cases} x_3 = \frac{y_b-(\tan\theta_b)x_b+(-\sec\theta_b-\sec\theta_a)\frac{\varphi_t}{2}}{\tan\theta_a-\tan\theta_b} \\ y_3 = (\tan\theta_a)x_3 + (\sec\theta_a)\frac{\varphi_t}{2} \end{cases} \tag{5}$$

$$\begin{cases} x_4 = \frac{y_b-(\tan\theta_b)x_b+(-\sec\theta_b+\sec\theta_a)\frac{\varphi_t}{2}}{\tan\theta_a-\tan\theta_b} \\ y_4 = (\tan\theta_a)x_4 - (\sec\theta_a)\frac{\varphi_t}{2}. \end{cases} \tag{6}$$

The region formed by (x_1, y_1), (x_2, y_2), (x_3, y_3), and (x_4, y_4) is a parallelogram, and its area A_{IR} is

$$A_{IR} = |D_1||D_2|\,|\sin(\theta_a - \theta_b)|$$

where D_1 and D_2 are two edges of the parallelogram. The lengths of $|D_1|$ and $|D_2|$ are

$$\begin{aligned} |D_1| &= \sqrt{(x_1-x_2)^2+(y_1-y_2)^2} \\ &= \sqrt{[1+(\tan\theta_b)^2]\left[\frac{(\sec\theta_a)\varphi_t}{\tan\theta_a-\tan\theta_b}\right]^2} \\ &= \frac{\sec\theta_a\sec\theta_b}{\tan\theta_a-\tan\theta_b}\varphi_t \\ |D_2| &= \sqrt{(x_2-x_4)^2+(y_2-y_4)^2} \\ &= \sqrt{[1+(\tan\theta_a)^2]\left[\frac{(\sec\theta_b)\varphi_t}{\tan\theta_a-\tan\theta_b}\right]^2} \\ &= \frac{\sec\theta_a\sec\theta_b}{\tan\theta_a-\tan\theta_b}\varphi_t. \end{aligned}$$

Because

$$\frac{1}{\tan\theta_a-\tan\theta_b} = \frac{\cos\theta_a\cos\theta_b}{\sin(\theta_a-\theta_b)}$$

the area is

$$\begin{aligned} A_{IR} &= \frac{\varphi_t^2}{[\sin(\theta_a-\theta_b)]^2}|\sin(\theta_a-\theta_b)| \\ &= \frac{\varphi_t^2}{\left|\cos\left(\frac{\pi}{2}-(\theta_a-\theta_b)\right)\right|}. \end{aligned} \tag{7}$$

To minimize the positioning error, we attempt to minimize A_{IR}. The parallelogram has the smallest area when the denominator of (7) is 1, i.e., $\cos(\pi/2-(\theta_a-\theta_b)) = 1$. In other words, the DEV that has a 90° or 270° transmission azimuth angle difference with the PNC is the best second anchor among all candidates. ■

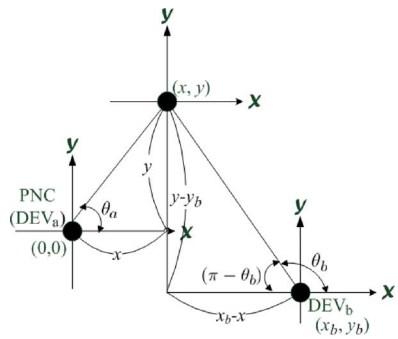

Fig. 3. Example of coordinate calculation for a new joining DEV when utilizing the OAP method.

Based on Proposition 1, we design the following two anchor pair selection mechanisms: 1) One_Anchor_Pair (OAP) and 2) All_Anchor_Pairs (AAP). OAP utilizes Proposition 1 to select the second anchor, whereas AAP utilizes Proposition 1 to do weight assignment.

1) *OAP.* Once a new DEV has finished the message exchanges of association request/reply with the PNC, all anchor candidates then transmit their information of coordinates and transmission azimuth angles to that new DEV. Among these anchor candidates, the new DEV selects the PNC and the anchor candidate that satisfies Proposition 1 to be its anchor pair. As shown in Fig. 3, let DEV_a and DEV_b denote two selected anchors. The coordinates of DEV_a and DEV_b are (0, 0) and (x_b, y_b), respectively, and the transmission azimuth angles of DEV_a and DEV_b are θ_a and θ_b, respectively. Let (x, y) denote the coordinate of this new DEV. Therefore, we know that

$$\begin{cases} \frac{y}{x} = \tan\theta_a \\ \frac{y-y_b}{x-x_b} = \tan\theta_b \end{cases}$$

and thus

$$\begin{cases} y = (\tan\theta_a)x \\ y = (\tan\theta_b)x + y_b - (\tan\theta_b)x_b. \end{cases}$$

After variable substitution, we derive

$$(x, y) = \left(\frac{y_b-(\tan\theta_b)x_b}{\tan\theta_a-\tan\theta_b}, \frac{(\tan\theta_a)y_b-(\tan\theta_a)(\tan\theta_b)x_b}{\tan\theta_a-\tan\theta_b}\right). \tag{8}$$

One illustrative example is shown in Fig. 4. Because DEV_c is the third node that joins this piconet, it can only select DEV_a and DEV_b as its anchors. In this example, we assume that θ_a and θ_b are 105° and 160°, respectively. The coordinate of DEV_b is (3.897, 2.25). Based on (8), the coordinate of DEV_c is (−1.089, 4.064).

Then, DEV_d joins the piconet, and we can choose either (DEV_a, DEV_b) or (DEV_a, DEV_c) as its anchor pair. The transmission azimuth angles of DEV_a and DEV_b to DEV_d are 45° and 145°, respectively. On the other hand, the transmission azimuth angles of DEV_a and

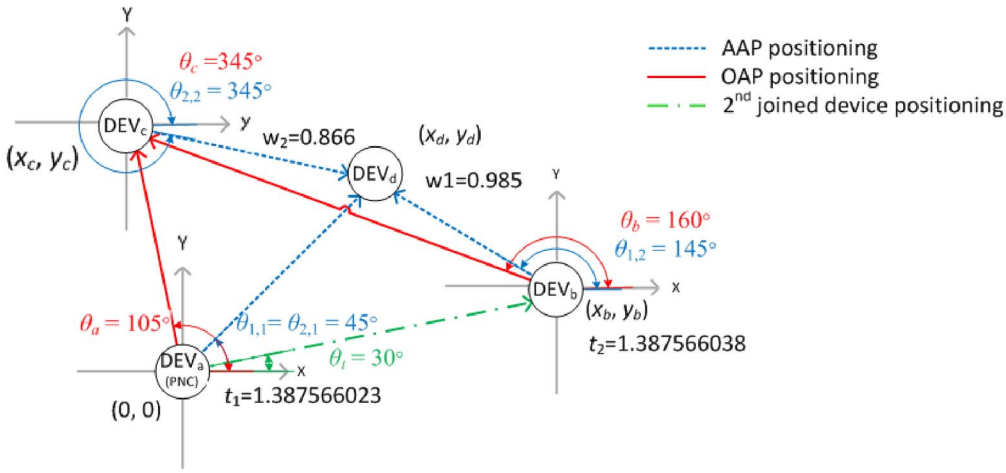

TDOA	Joined DEV	t_1	t_2	θ_t	Coordinates
	DEV$_b$(x_b, y_b)	1.387566023	1.387566038	30°	(3.897, 2.25)

OAP	Joined DEV	Anchor pair	Azimuth angle (θ_a, θ_b)	Coordinates
	DEV$_c$ (x_c, y_c)	(DEV$_a$, DEV$_b$)	(105°, 160°)	(-1.089, 4.064)
	DEV$_d$ (x_d, y_d)	(DEV$_a$, DEV$_b$)	(45°, 145°)	(2.975, 2.975)
	DEV$_d$ (x_d, y_d)	(DEV$_a$, DEV$_c$)	(45°, 345°)	(2.689, 2.689)

AAP	Joined DEV	Anchor pair	Azimuth angle	Temp_coordinates	Weight	Coordinates
	DEV$_c$ (x_c, y_c)	(DEV$_a$, DEV$_b$)	(105°, 160°)	(-1.089, 4.064)	1	(-1.089, 4.064)
	DEV$_d$ (x_d, y_d)	(DEV$_a$, DEV$_b$)	(45°, 145°)	(2.975, 2.975)	0.526	(2.839, 2.839)
		(DEV$_a$, DEV$_c$)	(45°, 345°)	(2.689, 2.689)	0.474	

Fig. 4. Coordinate calculation for DEV_c and DEV_d.

DEV_c to DEV_d are 45° and 345°, respectively. Because $|\theta_a - \theta_b| = 100°$ and $|\theta_a - \theta_c| = 300°$, (DEV_a, DEV_b) creates a smaller IR area than (DEV_a, DEV_c). Thus, DEV_d selects (DEV_a, DEV_b) to be its anchor pair, and its coordinate is (2.975, 2.975).

2) *AAP.* The basic idea of AAP is that, when utilizing as many anchor pairs as possible, the IR has the smallest area, and thus, the positioning error is the least. Thus, AAP considers all available anchor pairs to do positioning, and the PNC is the designated anchor of all pairs. Assume that one newly joining DEV has n anchor pairs. This DEV gets a coordinate from each anchor pair, and coordinate calculation is according to (6). Each coordinate is further assigned a weight based on the transmission azimuth angle difference of two anchors. The anchor pair whose difference of transmission azimuth angles is nearer 90° is assigned a larger weight. Therefore, the assigned weight of the kth anchor pair is

$$\omega_k = \frac{\sigma_k}{\sum_{i=1}^{n} \sigma_i}, k = 1, 2, \ldots, n \tag{9}$$

where $\sigma_k = |\cos(\pi/2 - (\theta_{k,2} - \theta_{k,1}))|$, and $\theta_{k,1}$ and $\theta_{k,2}$ are the transmission azimuth angles of the first and second anchors for the kth anchor pair, respectively. Let $(x_{k,2}, y_{k,2})$ be the coordinate of the second anchor of the kth anchor pair. Note that $(x_{k,1}, y_{k,1}) = (0, 0)$, because the PNC is always the first anchor of each pair.

By integrating (8) and (9), the coordinate of this newly joining DEV (x, y) is

$$(x, y) = \left(\sum_{k=1}^{n} \omega_k \frac{y_{k,2} - (\tan\theta_{k,2}) x_{k,2}}{\tan\theta_{k,1} - \tan\theta_{k,2}} \right. \\ \left. \sum_{k=1}^{n} \omega_k \frac{(\tan\theta_{k,1}) y_{k,2} - (\tan\theta_{k,1}\tan\theta_{k,2}) x_{k,2}}{\tan\theta_{k,1} - \tan\theta_{k,2}} \right). \tag{10}$$

Again, we use the same example (shown in Fig. 4) to explain the operations of AAP. Because DEV_c has only two anchor candidates DEV_a and DEV_b, its derived coordinate is $(-1.089, 4.064)$. On the other hand, DEV_d has two anchor pairs, i.e., (DEV_a, DEV_b) and (DEV_a, DEV_c). For the first anchor pair, $(\theta_{1,1}, \theta_{1,2}) = (45°, 145°)$. For the second anchor pair, $(\theta_{2,1}, \theta_{2,2}) = (45°, 345°)$. The coordinates that are derived from the two anchor pairs are (2.975, 2.975) and (2.689, 2.689), respectively. Furthermore, ω_1 is 0.526, and ω_2 is 0.473. Thus, the coordinate of DEV_d is $0.562 \times (2.975, 2.975) + 0.474 \times (2.689, 2.689) = (2.822, 2.822)$.

III. Channel Time Allocation Period-Minimized Scheduling Algorithm

In this section, we describe the proposed intrapiconet scheduling algorithm called CTAP-minimized scheduling. The

objective of the CTAP-minimized scheduling algorithm is to use the least channel time to serve all data flows such that the system throughput is maximized.

In the CTAP-minimized scheduling algorithm, topology and data flow information is represented by a two-layer flow graph $G = (V, E_1, E_2)$, where V is the set of n data flows $f_1, f_2, f_3, \ldots, f_{\mathrm{n}}$, and E_1 and E_2 are the sets of flow relation, $E_i \in V \times V$, $i = 1, 2$. Vertex v_i is represented as (f_i, t_i), where f_i and t_i are the flow ID and channel time requirement, respectively. The layer-1 edges $\forall e_i \in E_1$ are unidirectional, and the direction means the scheduling order of data flows. The layer-2 edges $\forall e_j \in E_2$ indicate the interference relation between any two flows, and thus, these edges are undirectional. In the following discussion, we use $v_i \cdot f$ and $v_i \cdot t$ to indicate the represented flow ID and the channel time requirement of vertex i, respectively. In addition, $e_1^{\vec{ij}}$ and e_2^{ij} indicate the layer-1 and layer-2 edges between vertices i and j.

CTAP-minimized scheduling consists of the following three phases: 1) *layer-1 edge construction*; 2) *layer-2 edge construction*; and 3) *scheduling*. Each phase is described as follows.

A. Phase 1: Layer-1 Edge Construction

In the CTAP-minimized scheduling algorithm, flows are sorted in decreasing order of requested channel time. Based on the sorting result, vertices and the corresponding layer-1 graph are obtained. In particular, let $(f_{1^*}, f_{2^*}, f_{3^*}, \ldots, f_{n^*})$ be the sorting result that satisfies $t_{1^*} \geq t_{2^*} \geq t_{3^*} \geq \ldots \geq t_{n^*}$. Next, the n vertices are $(f_{1^*}, t_{1^*}), (f_{2^*}, t_{2^*}), (f_{3^*}, t_{3^*}), \ldots, (f_{n^*}, t_{n^*})$. Because this sequence indicates the scheduling order, each vertex has an edge to its right-hand-side neighbor, i.e., $e_1^{\vec{ij}}, i = 1, 2, , n-1, j = i+1$. Here, $\vec{ij}$ indicates that the edge direction is from vertex i to vertex j.

B. Phase 2: Layer-2 Edge Construction

The layer-2 graph represents the possibilities of spatial channel reuse. An edge between two vertices is added when these two flows interfere with each other upon simultaneous transmission, and thus, they cannot be scheduled in the same CTA. Because of equipping a directional antenna, a receiver only accepts signals in a certain beam direction. In this paper, we call this beam pattern *reception beam*, and its beamwidth is denoted as φ_r.

Let (s_i, r_i) and (s_j, r_j) be the senders and receivers of flows f_i and f_j, respectively Our concepts of exploring the possibility of spatial channel reuse for f_i and f_j are twofold.

1) If s_i (or s_j) is not located in r_j's (or r_i's) reception beam, it is obvious that r_j (or r_i) cannot hear signals that are sent from s_i (or s_j), and thus, f_i and f_j do not interfere with each other.
2) If s_i (or s_j) is located in r_j's (or r_i's) reception beam and r_j (or r_i) is located in s_i (or s_j) transmission beam, r_j (or r_i) can hear signals from s_i (or s_j). Consequently, f_i and f_j interfere with each other and cannot be scheduled in the same CTA.

Before explaining the verification rules of spatial channel reuse in detail, we first define the following two parameters.

1) *Reception azimuth angle* (θ_r): This is the angle between the direction of the reception beam and the x-axis in the azimuth plane.
2) $\Delta\theta_z^{x,y}$: This is the included angle of two vectors $\vec{zx}$ and $\vec{zy}$. According to the trigonometric function, we have

$$\Delta\theta_z^{x,y} = \cos^{-1}\left(\frac{\vec{zx} \cdot \vec{zy}}{\mid \vec{zx} \mid\mid \vec{zy} \mid}\right). \tag{11}$$

For flows f_i and f_j, because their coordinates are known, we can derive four included angles—$\Delta\theta_{r_i}^{s_i,s_j}$, $\Delta\theta_{r_j}^{s_i,s_j}$, $\Delta\theta_{s_i}^{r_i,r_j}$, and $\Delta\theta_{s_j}^{r_i,r_j}$—according to (11).

Flow f_j cannot simultaneously transmit data with f_i when either r_j can receive s_i's signals or r_i can receive s_j's signals. Moreover, r_j can receive s_i's signals only when the following two conditions are satisfied: 1) s_i is located within the reception beam of r_i, and 2) r_j is located within the transmission beam of s_i. For condition 1, the induced angle $\Delta\theta_{r_j}^{s_i,s_j}$ must be less than or equal to half the reception beamwidth. For condition 2, the induced angle $\Delta\theta_{s_i}^{r_i,r_j}$ must be less than or equal to half the transmission beamwidth. However, we consider the effect of sidelobes; thus, the angle requirement is doubled to be φ_r and φ_t.

Similarly, to receive s_j's signals, r_i must be located within the transmission beam of s_j, and s_j must be located within the reception beam of r_i. Therefore, the induced angles $\Delta\theta_{r_i}^{s_i,s_j}$ and $\Delta\theta_{s_j}^{r_i,r_j}$ must be less than or equal to the reception and the transmission beamwidths, respectively.

Based on the aforementioned description, the layer-2 edge construction rule is given as follows.

Layer-2 edge construction rule:

For vertices (f_i, t_i) and (f_j, t_j)

If

$$\left(\left(\Delta\theta_{r_j}^{s_j,s_i} \leq \varphi_r\right) \&\& \left(\Delta\theta_{s_i}^{r_i,r_j} \leq \varphi_t\right)\right) \Big\| \left(\left(\Delta\theta_{r_i}^{s_i,s_j} \leq \varphi_r\right) \&\& \left(\Delta\theta_{s_j}^{r_j,r_i} \leq \varphi_t\right)\right)$$

Then

$$\exists e_2^{ij};$$

Else

$$\nexists e_2^{ij}.$$

This construction rule is applied to all pairwise vertices. Then, the 2-layer flow graph is constructed.

C. Scheduling

After constructing both layer-1 and layer-2 edges, the PNC then performs scheduling by visiting all vertices of the constructed flow graph in sequence. Let S be the set that consists

of all flows and S_i be the subset of flows that are scheduled in CTA$_i$. Initially, S_i is an empty set. The PNC first visits the entrance vertex of the first-layer flow graph (i.e., v_1), schedules $v_1 \cdot f$ in CTA$_1$, sets the time duration of CTA$_1$ to be $v_1 \cdot t$, and then moves $v_1 \cdot f$ from S to S_1. The PNC further visits the second vertex v_2 and checks if e_2^{12} exists. If e_2^{12} exists, the PNC allocates CTA$_2$ to $v_2 \cdot f$, sets the time duration to be $v_2 \cdot t$, and moves $v_2 \cdot f$ from S to S_2; otherwise, $v_2 \cdot f$ is scheduled in CTA$_1$, and $v_2 \cdot f$ is moved from S to S_1. Assume that $v_2 \cdot f$ is scheduled in CTA$_1$. The PNC then verifies the possibility of the concurrent transmission of $v_3 \cdot f$ and S_1. If both e_2^{13} and e_2^{23} do not exist, then $v_3 \cdot f$ is also scheduled in CTA$_1$. When S is empty, the scheduling stops.

Assume that there are m flow subsets. Let $V(S_i)$ and T_i be the vertices in S_i and the time duration of CTA$_i$, respectively, and $1 \leqq i \leqq m$. In addition, $T_1 \geqq T_2 \geqq \ldots \geqq T_m$. For flow f_k, the PNC keeps trying to schedule f_k in CTA$_i$, $i = 1, 2, 3, \ldots, m$ by verifying the existence of layer-2 edges. The PNC stops its discovering when a CTA, e.g., CTA$_j$ and $1 \leqq i \leqq m$, can accommodate f_k without interfering with all existing flows. If f_k cannot be scheduled in one of these m CTAs, the PNC allocates a new CTA, i.e., CTA$_{(m+1)}$, to f_k, and sets T_{m+1} to be t_k. The scheduling rule is summarized as follows.

Scheduling rules:

For f_k
  If $(\nexists e_2^{kl}, \forall l\ S_i, i \in 1, 2, \ldots, m)$
  Then schedule f_k in CTA$_i$ without modifying T_i;
  Else schedule f_k in CTA$_{(m+1)}$ and set $T_{m+1} = t_k$.

We use an example to illustrate the operations of CTAP-minimized scheduling. In Fig. 5, there are eight DEVs $(s_1 \sim s_4, r_1 \sim r_4)$ and four flows $f_1(s_1 \rightarrow r_1)$, $f_2(s_2 \rightarrow r_2)$, $f_3(s_3 \rightarrow r_3)$ and $f_4(s_4 \rightarrow r_4)$. The required transmission times of the four flows are 0.7, 0.4, 0.8, and 0.5 ms, respectively. The network topology and flow information are summarized in Fig. 5(a). Both transmission and reception beamwidths are set to be 30°. An arc indicates the transmission beam pattern of a sender, and a colored triangle represents the reception beam pattern of a receiver. The PNC of this network is s_4.

First, because the time requirements of four flows are 0.7, 0.4, 0.8, and 0.5 ms, respectively, the vertices, after sorting in decreasing order of time demand, are $v_1(f_3, 0.8)$, $v_2(f_1, 0.7)$, $v_3(f_4, 0.5)$, and $v_4(f_2, 0.4)$, respectively, as shown in Fig. 5(b). Then, each vertex has an outbound arrowed edge to its right-hand-side neighbor. Now, we have constructed the layer-1 flow graph.

Next, the interference relation of any two vertices is discovered by performing phase-2 operations. The included angles of all flow pairs are listed in Fig. 5(a). We first verify the interference relation between vertices v_1 and v_2. Based on Fig. 5(a), we know that $\Delta\theta_{s_3}^{r_3,r_1} = 10°$, $\Delta\theta_{r_3}^{s_3,s_1} = 15°$, $\Delta\theta_{s_1}^{r_1,r_3} = 8°$, and $\Delta\theta_{r_1}^{s_1,s^3} = 15°$. Because f_1 and f_3 satisfy two conditions—$(\Delta\theta_{r_3}^{s_3,s_1} = 15°) \leq (\varphi_r = 30°)$ and $(\Delta\theta_{s_1}^{r_1,r^3} = 8°) \leq (\varphi_t = 30°)$—a layer-2 edge e_2^{12} exists between v_1 and v_2.

We further verify the interference relation between vertices v_1 and v_3. Because both $\Delta\theta_{s_3}^{r_3,r_4} = 88°$ and $\Delta\theta_{s_4}^{r_4,r_3} = 104°$ are larger than transmission beamwidth $(\varphi_t = 30°)$, no layer-2 edge exists between v_1 and v_3. After pairwise verification, the layer-2 flow graph is constructed, as shown in Fig. 5(b).

The last phase is scheduling. The PNC sequentially visits all vertices. It first visits vertex v_1, allocates CTA$_1$ to f_3, and sets CTA$_1$'s time duration to be 0.8 ms. Following the $e_1^{\vec{12}}$ edge, the PNC then visits v_2. Because there is a layer-2 edge e_2^{12} between v_1 and v_2, the PNC allocates a new CTA (i.e., CTA$_2$) to f_1 and sets the time duration to 0.7 ms. Again, the PNC follows the $e_1 \vec{23}$ edge and visits v_3. Because e_2^{41} does not exist, f_4 is scheduled in CTA$_1$, whereas the CTA$_1$ time duration remains intact. Finally, the PNC visits v_4 and discovers that f_2 does not interfere with both f_3 and f_4, because both e_2^{23} and e_2^{24} do not exist. Thus, the PNC again schedules f_2 in CTA$_1$ without modifying the CTA$_1$ time duration. In short, v_1, v_3, and v_4 can be processed in CTA$_1$, because no interference exists, whereas v_2 is scheduled in CTA$_2$, because it interferes with v_1.

The total CTAP time to serve these four flows is $(0.8 \text{ ms} + 0.7 \text{ ms}) = 1.5$ ms, as shown in Fig. 5(c). Compared with the conventional scheduling that uses $(0.8 \text{ ms} + 0.7 \text{ ms} + 0.5 \text{ ms} + 0.4 \text{ ms}) = 2.4$ ms, the improvement of channel time utilization of CTAP-minimized scheduling is up to 37.5%.

Given correct topology information and flow information, CTAP-minimized scheduling utilizes the least channel time to serve all data flows, as stated in Proposition 2.

Proposition 2: Let S be the set of n flows. S is sorted in decreasing order of channel time requirement. Let T be the required channel time to serve these n flows upon utilizing the CTAP-minimized scheduling approach. Then, T is the least channel time to serve these n flows.

Proof: We utilize the apagoge method to prove Proposition 2. Assume that these n flows are scheduled in m CTAs. Let CTA$_i$ denote the ith CTA. T_i and S_i indicate the time duration of CTA$_i$ and the subset of flows scheduled in CTA$_i$, respectively. Let f_{ij} and t_{ij} be the jth flow scheduled in CTA$_i$ and its channel time requirement, respectively. Based on CTAP-minimized scheduling, we know that

$$\begin{cases} T_i = t_{i1} \\ T_1 \geq T_2 \geq \ldots \geq T_m \\ T = \sum_{k=1}^{m} T_k. \end{cases}$$

If T is not the least channel time to serve all flows, there is at least one CTA that can be shortened. Let the total service time and the ith CTA time, after rescheduling, be T^* and T_i^*. Thus

$$T > \left(T^* = \sum_{k=1}^{m} T_k^* \right).$$

Suppose that CTA$_i$ can be shortened. This condition means that f_{i1} must be rescheduled to CTA$_h$, $1 \leq h \leq (i-1)$. However, the reason that f_{i1} cannot be scheduled in CTA$_h$ is that f_{i1} fails the concurrent transmission verification with S_h, $1 \leq h \leq (i-1)$. If f_{i1} is rescheduled to CTA$_h$, some flows

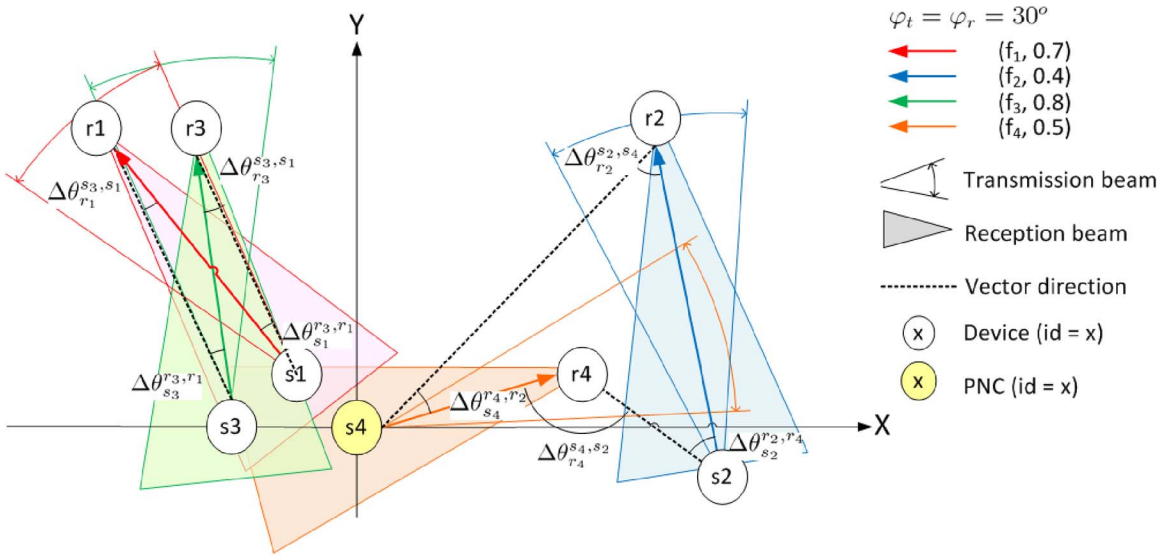

Flow id	(sender, receiver)	Required transmission time	Included angle			
			flow1	flow2	flow3	flow4
f_1	(s1, r1)	0.7 ms	-	$\Delta\theta_{s_1}^{r_1,r_2} = 90°$	$\Delta\theta_{s_1}^{r_1,r_3} = 8°$	$\Delta\theta_{s_1}^{r_1,r_4} = 135°$
			-	$\Delta\theta_{r_1}^{s_1,s_2} = 25°$	$\Delta\theta_{r_1}^{s_1,s_3} = 15°$	$\Delta\theta_{r_1}^{s_1,s_4} = 5°$
f_2	(s2, r2)	0.4 ms	$\Delta\theta_{s_2}^{r_2,r_1} = 51°$	-	$\Delta\theta_{s_2}^{r_2,r_3} = 46°$	$\Delta\theta_{s_2}^{r_2,r_4} = 43°$
			$\Delta\theta_{r_2}^{s_2,s_1} = 65°$	-	$\Delta\theta_{r_2}^{s_2,s_3} = 65°$	$\Delta\theta_{r_2}^{s_2,s_4} = 55°$
f_3	(s3, r3)	0.8 ms	$\Delta\theta_{s_3}^{r_3,r_1} = 10°$	$\Delta\theta_{s_3}^{r_3,r_2} = 60°$	-	$\Delta\theta_{s_3}^{r_3,r_4} = 88°$
			$\Delta\theta_{r_3}^{s_3,s_1} = 15°$	$\Delta\theta_{r_3}^{s_3,s_2} = 50°$	-	$\Delta\theta_{r_3}^{s_3,s_4} = 21°$
f_4	(s4, r4)	0.5 ms	$\Delta\theta_{s_4}^{r_4,r_1} = 118°$	$\Delta\theta_{s_4}^{r_4,r_2} = 28°$	$\Delta\theta_{s_4}^{r_4,r_3} = 104°$	-
			$\Delta\theta_{r_4}^{s_4,s_1} = 14°$	$\Delta\theta_{r_4}^{s_4,s_2} = 135°$	$\Delta\theta_{r_4}^{s_4,s_3} = 5°$	-

(a)

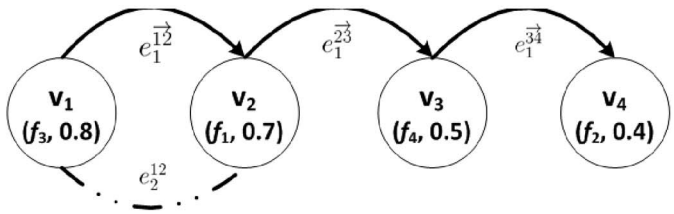

(b)

Conventional Scheduling			
CTA1 (0.7 ms)	CTA2 (0.4 ms)	CTA3 (0.8 ms)	CTA4 (0.5 ms)
(f_1, 0.7)	(f_2, 0.4)	(f_3, 0.8)	(f_4, 0.5)

CTAP-minimized Scheduling	
CTA1 (0.8 ms)	CTA2 (0.7 ms)
v_1 (f_3, 0.8)	v_2 (f_1, 0.7)
v_3 (f_4, 0.5)	
v_4 (f_2, 0.4)	

(c)

Fig. 5. CTAP-minimized scheduling. (a) Network topology and flow information. (b) Constructed two-layer flow graph. (c) Scheduling results of conventional scheduling and CTAP-minimized.

in CTA_h must be rescheduled to other CTAs. We consider following two possibilities.

1) $t_{h1} > t_{h2} > t_{i1} > t_{h3}$. f_{i1} interferes with f_{h1} or f_{h2}. To allocate f_{i1} in CTA_h, either f_{h1} or f_{h2} must be rescheduled to CTA_i. When allocating f_{h1} to CTA_i, T_h^* and $T_i^* = T_h$. Thus, $T^* = T$, which contradicts our assumption.

On the other hand, f_{h2} is allocated to CTA_i, and f_{i1} is scheduled in CTA_h. In such a situation, $T_h^* = T_h = t_{h1}$, and $T_i^* = t_{h2} > T_i$. Thus, $T < T^*$, which also contradicts our assumption.

2) $t_{h1} > t_{i1} > t_{h2}$. The only way of scheduling f_{i1} in CTA_h is to allocate f_{h1} to other CTAs. Similar to the first case, we know that $T \leq T^*$.

TABLE I
NOTATION LIST

Notation	Meaning
n_s	The number of superframes to schedule all data flows
m_i	The number of CTAs in the i^{th} superframe
$n_{i,j}$	The number of data flows allocated in the j^{th} CTA of the j^{th} superframe
t_b	Beacon duration
t_c	CAP time duration
t_m	MCTA time duration
Δ_t	Interframe guard time
$t_{i,j}$	The j^{th} CTA time duration of the i^{th} frame
$S_{i,j}$	The set of flows that are scheduled in the j^{th} CTA of the j^{th} superframe
$\mid S_{i,j} \mid$	The number of flows in set $S_{i,j}$
$t(f_{i,j,k})$	The channel time requirement of the k^{th} flow in the j^{th} CTA of the i^{th} superframe
t^j_{CTAP}	The CTAP duration of the j^{th} superframe

TABLE II
PARAMETER SETTINGS

Parameter	Value
Piconet area	10 m × 10 m
Number of devices	25
Beam width	0°~90°
Beacon period	1 ms
CAP duration	2 ms
MCTA duration	0.3 ms
Guard time	25 ns
Superframe maximal length	20 ms
Flow transmission time	0.1 ~ 1 ms

As a result, T cannot be shortened, and CTAP-minimized scheduling utilizes the least time to serve these n flows. ■

IV. PERFORMANCE EVALUATION

In this section, we evaluate the proposed scheduling algorithm by developing simulation results. We first describe our simulation environment and performance metrics and then discuss simulation results.

A. Simulation Environment

The piconet topology is randomly generated in a 10 m × 10 m area. The first joining DEV is designated to serve as a PNC. The maximum duration of a superframe is 20 ms, whereas it varies according to the time requests of data flows. The packet arrival of a DEV is a Poisson distribution with rate λ. The simulated channel model is as described in [25], which is specific to 60-GHz wireless systems. The notation and parameter settings in our experiments are listed in Tables I and II, respectively. Each simulation result is the average of 50 experiments.

We compare the performance of the following four scheduling algorithms:

1) CTAP-minimized;
2) conventional scheduling;
3) FIFO with spatial–temporal channel reuse, which is called first-in first-out (FIFO) here);
4) DTS [22].

The operations of FIFO are similar to CTAP-minimized scheduling, except that it does not execute channel time sorting. Instead, flows are served according to their arrival time.

The performance metrics are described as follows.

1) *Utilized channel time* T: The utilized channel time to schedule all flows, which is calculated as

$$T = n_s(t_b + t_c + t_m + 3\Delta_t) + \sum_{i=1}^{n_s}\left[\sum_{j=1}^{m_i}(t_{i,j} + \Delta_t)\right].$$

2) *System throughput* ρ: The aggregated transmission rate of a piconet. Its unit is given in gigabits per second. When all DEVs have utilized the same transmission rate r Gb/s, the system throughput is

$$\rho = \frac{r\sum_{i=1}^{n_s}\sum_{j=1}^{m_i}\sum_{k=1}^{|S_{i,j}|} t(f_{i,j,k})}{T}$$

where T is the utilized channel time.

3) *Scheduling efficiency* (δ): The percentage of collided channel time, which is caused by positioning errors. It is derived by

$$\delta = 1 - \frac{T_c}{T}$$

where T_c is the total time duration of collided CTAs, and T is the utilized channel time.

4) *Spatial channel reuse degree* (γ): The number of scheduled data flows per data transmission time unit (in milliseconds). Its definition is

$$\gamma = \frac{1}{n_s m_i}\sum_{i=1}^{n_s}\sum_{j=1}^{m_i}\frac{n_{i,j}}{t_{i,j}}.$$

B. Simulation Results

We then present and discuss the simulation results of each observed metric.

1) *Utilized channel time*. Fig. 6 shows the utilized channel time of each approach. For FIFO and CTAP-minimized scheduling, we implement the following three positioning mechanisms: 1) ideal; 2) OAP; and 3) AAP. The ideal positioning means that the exact coordinates of all DEVs are known; thus, there is no positioning error. In this simulation, we set $\varphi_t = \varphi_r = 30°$. Obviously, the conventional scheduling uses the most channel time among four mechanisms to schedule all flows, because each CTA is allocated to exact one flow. DTS, on the other hand, uses more channel time than CTAP-minimized scheduling and FIFO. The reason is that the verification rule of spatial channel reuse of DTS is relatively conservative. Some flows that can simultaneously transmit data may fail the verification test. Although implementing

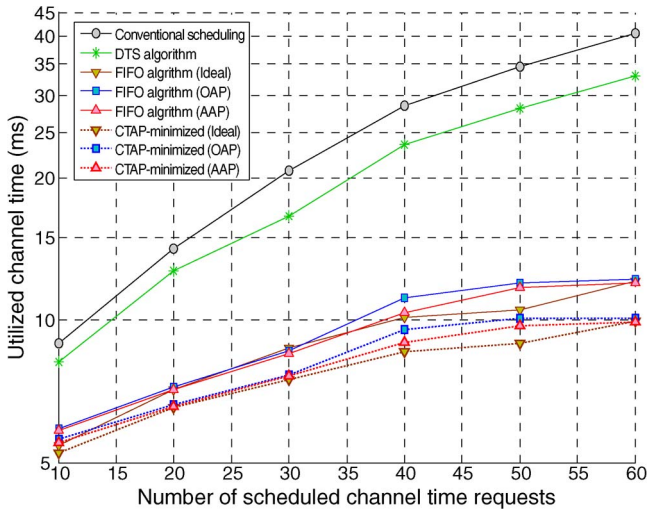

Fig. 6. Utilized channel time versus the number of data flows for $\varphi_t = \varphi_r = 30^\circ$ and $\lambda = 0.8$.

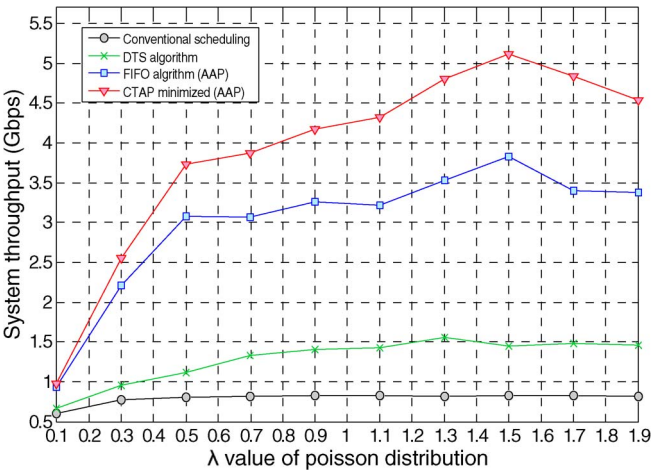

Fig. 7. Throughput performance versus various λ settings for $\varphi_t = \varphi_r = 30^\circ$.

the same verification rules, FIFO still performs worse than CTAP-minimized. This case reveals the effect of sorting data flows in decreasing order of channel time requirement. Compared with ideal positioning, the max and min performance degradation of CTAP-minimized with implementing AAP and OAP is (8.6%, 0.2%) and (11.9%, 1.7%), respectively.

2) *System throughput*. We investigate the performance of system throughput, and the result is shown in Fig. 7. Because each CTA is exclusive to a flow when implementing the conventional scheduling protocol, its throughput is intact. DTS uses neighbor profiles to explore noninterfered flows and schedule the channel time; thus, a PNC may schedule multiple data flows in a CTA. As a result, DTS outperforms the conventional scheduling protocol. Due to providing coordinate information to the PNC, CTAP-minimized performs even better than DTS. Compared with CTAP-minimized and as expected, FIFO has lower throughputs with different λ values. The only difference between FIFO and CTAP-minimized is whether to perform sorting flows in decreasing order of channel time requirement. Based on Proposition 2, the total used channel time could be shortened without sorting flows.

When λ increases from 0.1 to 0.5, we observe that the system throughput significantly increases for both FIFO and CTAP-minimized. The reason is that a superframe can accommodate all packets. As λ keeps increasing, both approaches utilize more superframes to deliver data packets, and thus, the system throughput slowly increases. Interestingly, when λ is larger than 1.5, the system throughput decreases. The reason is the high collision probability of transmitting channel time requests.

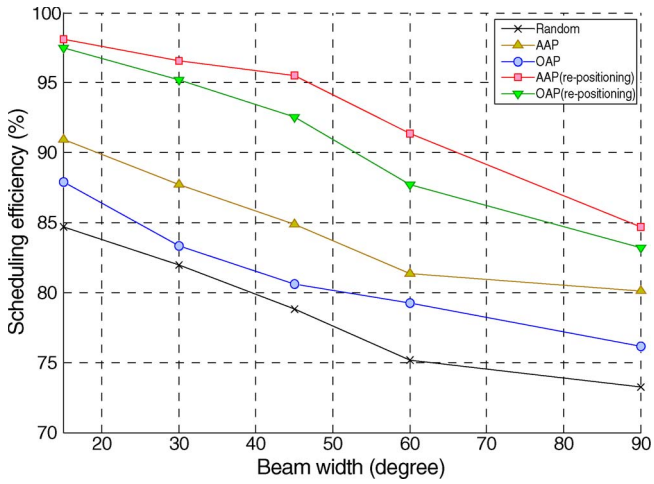

Fig. 8. Performance of scheduling efficiency versus various beamwidth settings for CTAP-minimized with different positioning schemes.

3) *Scheduling efficiency*. Once the coordinates of DEVs have inaccurately been estimated, the collision may happen in CTAs due to being scheduled inaccurate topology information. To observe the relation between beamwidth and wasted channel time caused by an inaccurate positioning result, we compare five positioning approaches, i.e., random, AAP, OAP, AAP (repositioning), and OAP (repositioning). *Random* means that, instead of obeying Proposition 1, every DEV randomly selects its second anchor. Regardless of adopting OAP or AAP, the third joining DEV only have two available anchors. These two anchors may result in a large IR area and a high positioning error. In such a situation, this positioning error will impact the following positioning accuracy and scheduling performance. We call this condition the *propagation effect of positioning error*. AAP (repositioning) and OAP (re-positioning) are two enhanced positioning schemes that deal with the propagation effect of positioning error. The main concept is that a PNC issues a repositioning command to all DEVs while changing the order to reduce positioning errors. The repositioning operations are out of the scope of this paper.

The performance of scheduling efficiency as a function of various beamwidth settings for the five positioning approaches is shown in Fig. 8. As expected, regardless of the positioning scheme used, the scheduling efficiency decreases as the beamwidth increases. Among all the approaches, the random scheme performs the

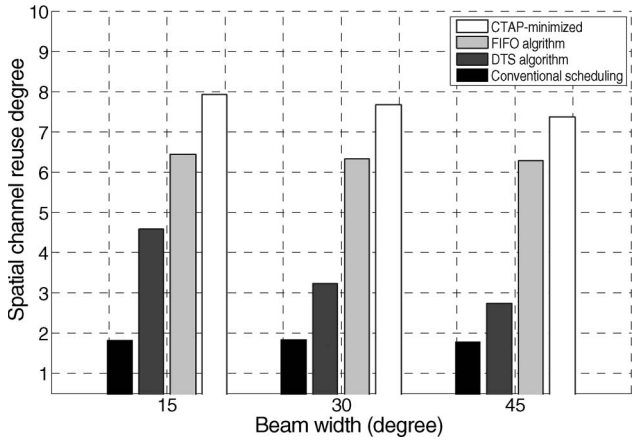

Fig. 9. Performance of scheduling efficiency versus various beamwidth settings for CTAP-minimized with different positioning schemes.

worst (when $\varphi_t = 60^\circ$, 25% channel time is wasted). The reason is that randomly choosing an anchor results in serious positioning inaccuracy. Compared with OAP, AAP has a smaller IR area and thus performs better in terms of scheduling efficiency. In addition, both AAP (repositioning) and OAP (repositioning) have around a 10% improvement. That is, CTAP-minimized scheduling can achieve higher performance when strengthening the positioning algorithm.

4) *Spatial channel reuse degree*. CTAP-minimized, FIFO, and DTS mechanisms improve the spatial channel reuse degree by allocating multiple flows in a CTA. Generally, the more the data flows in a CTA, the more the improvement in channel reuse.

Fig. 9 depicts the performance of the spatial channel reuse degree as the beamwidth increases from 15° to 45°. Because the conventional scheduling protocol does not allocate multiple noninterfering data flows in a CTA, its reuse degree is intact. On the other hand, when the beamwidth increases, the reuse degrees of the other three approaches decrease. Among the three approaches, DTS degrades the most (38%). The main reason is that DTS executes concurrent transmission validations based on the information of blocked sectors, which are recorded in neighbor profiles. However, the area of blocked sectors has a strong correlation with beamwidth. Indeed, as the beamwidth increases, the blocked area increases. Flows in the blocked area are not allowed to simultaneously transmit data, even if these flows do not interfere with one another. That is, the effect of spatial channel reuse is restricted by a large beamwidth. On the contrary, CTAP-minimized explores noninterfering flows through estimated coordinates and included angles. Although the IR area increases as the beamwidth increases, either properly selecting the second anchor or implementing AAP can minimize this impact. The simulation result shows that the degradation of spatial channel reuse degree for CTAP-minimized is less than $(7.93 - 7.27)/7.93 = 8.32\%$.

Although the performance variance of FIFO is the least among the three enhanced scheduling algorithms, we observe that sorting flows in decreasing order of time demand still affects spatial channel reusability.

V. Conclusion

In this paper, we have proposed a scheduling algorithm for IEEE 802.15.3c WPANs. Due to the characteristic of utilizing beamforming antennas, axis alignment and coordinate estimation are two essential factors for the design of spatial and directional reuse improved scheduling. We observe that azimuth angles and beamwidths impact the accuracy of coordinate estimation and coordinate accuracy further affects the scheduling efficiency of PNCs. We have designed two location determination schemes OAP and AAP, both of which try to reduce positioning errors. Upon collecting coordinates and transmission requests of DEVs, a PNC schedules noninterfered flows in the same CTA and sets the CTA time duration as the longest requesting time. The simulation results show that our mechanism improves scheduling efficiency. Our future work will extend this algorithm to support interpiconet scheduling.

References

[1] *IEEE Draft Amendment to IEEE Standard for Information Technology—Telecommunications and Information Exchange Between Systems—Local and Metropolitan Area Networks-Specific Requirements—Part 15.3: Wireless Medium Access Control (MAC) and Physical Layer (PHY) Specifications for High Rate Wireless Personal Area Networks (WPANs) Amendment 2: Millimeter-Wave Based Alternative Physical Layer Extension*, IEEE Unapproved Draft Std. P802.15.3c/D08, Mar. 2009.

[2] Z. Lan, C. Pyo, F. Kojima, H. Harada, and S. Kato, "On-demand device discovery enhancement of IEEE802.15.3 MAC for 60-GHz WPAN system," in *Proc. IEEE Pers., Indoor, Mobile Radio Commun.*, Sep. 2008, pp. 1–6.

[3] T. Ueda, K. Sugiyama, H. Iwai, S. Obana, and S. Bandyopadhyay, "Direction and communication-aware directional MAC protocol in ad hoc networks using directional antenna," in *Proc. IEEE Pers., Indoor, Mobile Radio Commun.*, Sep. 2006, pp. 1–5.

[4] G. Jakllari, W. Luo, and S. V. Krishnamurthy, "An integrated neighbor discovery and MAC protocol for ad hoc networks using directional antennas," *IEEE Trans. Wireless Commun.*, vol. 6, no. 3, pp. 1114–1124, Mar. 2007.

[5] D. Niculescu and B. Nath, "Ad hoc positioning system (APS) using AOA," in *Proc. 22nd IEEE INFOCOM*, Mar. 2003, vol. 3, pp. 1734–1743.

[6] J. Xu, M. Ma, and C. L. Law, "AOA cooperative position localization," in *Proc. IEEE Global Telecommun. Conf.*, Nov. 2008, pp. 1–5.

[7] J.-Y. Lee and R. A. Scholtz, "Ranging in a dense multipath environment using an UWB radio link," *IEEE J. Sel. Areas Commun.*, vol. 20, no. 9, pp. 1677–1683, Dec. 2002.

[8] P. Radosavljevic, Y. Guo, and J. Cavallaro, "Probabilistically bounded soft sphere detection for MIMO-OFDM receivers: Algorithm and system architecture," *IEEE J. Sel. Areas Commun.*, vol. 27, no. 8, pp. 1318–1330, Oct. 2009.

[9] L. B. Agudelo and A. N. Cadavid, "A novel correlation adaptive receiver structure for high speed transmissions in ultra wide band systems with realistic channel estimation," *IEEE J. Sel. Areas Commun.*, vol. 27, no. 8, pp. 1341–1346, Oct. 2009.

[10] S. Pinel, P. Sen, S. Sarkar, B. Perumana, D. Dawn, D. Yeh, F. Barale, M. Leung, E. Juntunen, P. Vadivelu, K. Chuang, P. Melet, G. Iyer, and J. Laskar, "60-GHz single-chip CMOS digital radios and phased-array solutions for gaming and connectivity," *IEEE J. Sel. Areas Commun.*, vol. 27, no. 8, pp. 1347–1357, Oct. 2009.

[11] F. Gutierrez, K. Parrish, and T. S. Rappaport, "On-chip integrated antenna structures in CMOS for 60-GHz WPAN systems," in *Proc. IEEE Global Telecommun. Conf.*, Nov. 2009, pp. 1–7.

[12] J. Wang, Z. Lan, C.-W. Pyo, T. Baykas, C.-S. Sum, M. A. Rahman, J. Gao, R. Funada, F. Kojima, H. Harada, and S. Kato, "Beam-codebook-based beamforming protocol for multi-Gbps millimeter-wave WPAN systems," *IEEE J. Sel. Areas Commun.*, vol. 27, no. 8, pp. 1390–1399, Oct. 2009.

[13] S. Yoon, T. Jeon, and W. Lee, "Hybrid beamforming and beamswitching for OFDM-based wireless personal area networks," *IEEE J. Sel. Areas Commun.*, vol. 27, no. 8, pp. 1425–1432, Oct. 2009.

[14] C.-S. Sum, R. Funada, J. Wang, T. Baykas, M. A. Rahman, and H. Harada, "Error performance and throughput evaluation of a multi-Gbps millimeter-wave WPAN system in the presence of adjacent and cochannel interference," *IEEE J. Sel. Areas Commun.*, vol. 27, no. 8, pp. 1433–1442, Oct. 2009.

[15] M. Lei, C.-S. Choi, R. Funada, H. Harada, and S. Kato, "Throughput comparison of multi-Gbps WPAN (IEEE 802.15.3c) PHY layer designs under nonlinear 60-GHz power amplifier," in *Proc. IEEE Pers., Indoor, Mobile Radio Commun.*, Sep. 2007, pp. 1–5.
[16] W. P. Chang and H. Harada, "Throughput analysis and improvement of hybrid multiple access in IEEE 802.15.3c mm-wave WPAN," *IEEE J. Sel. Areas Commun.*, vol. 27, no. 8, pp. 1414–1424, Oct. 2009.
[17] M. Park and P. Gopalakrishnan, "Analysis on spatial reuse and interference in 60-GHz wireless networks," *IEEE J. Sel. Areas Commun.*, vol. 27, no. 8, pp. 1443–1452, Oct. 2009.
[18] J. Shen, I. Nikolaidis, and J. Harms, "WLC25-4: Dynamic 802.15.3 WPAN scheduling using maximal matching," in *Proc. IEEE Global Telecommun. Conf.*, Nov. 2006, pp. 1–6.
[19] Z. Lan, C.-S. Sum, J. Wang, T. Baykas, F. Kojima, H. Nakase, and H. Harada, "Relay with deflection routing for effective throughput improvement in Gbps millimeter-wave WPAN systems," *IEEE J. Sel. Areas Commun.*, vol. 27, no. 8, pp. 1453–1465, Oct. 2009.
[20] C.-S. Sum, Z. Lan, R. Funada, J. Wang, T. Baykas, M. Rahman, and H. Harada, "Virtual time-slot allocation scheme for throughput enhancement in a millimeter-wave multi-Gbps WPAN system," *IEEE J. Sel. Areas Commun.*, vol. 27, no. 8, pp. 1379–1389, Oct. 2009.
[21] L. X. Cai, L. Cai, X. Shen, and J. W. Mark, "REX: A randomized exclusive region based scheduling scheme for mmWave WPANs with directional antenna," *IEEE Trans. Wireless Commun.*, vol. 9, no. 1, pp. 113–121, Jan. 2010.
[22] X. An and R. Hekmat, "Directional MAC protocol for Millimeter Wave based wireless personal area networks," in *Proc. IEEE Veh. Technol. Conf.—Spring*, May 2008, pp. 1636–1640.
[23] H. Xu, V. Kukshya, and T. S. Rappaport, "Spatial and temporal characteristics of 60-GHz indoor channels," *IEEE J. Sel. Areas Commun.*, vol. 20, no. 3, pp. 620–630, Apr. 2002.
[24] P. F. M. Smulders, "Statistical characterization of 60-GHz indoor radio channels," *IEEE Trans. Antennas Propag.*, vol. 57, no. 10, pp. 2820–2829, Oct. 2009.
[25] A. Maltsev, V. Erceg, E. Perahia, C. Hansen, R. Maslennikov, A. Lomayev, A. Strastyanov, and A. Khoryaev, *Channel Models for 60 GHz WLAN Systems*, IEEE doc.802.11-09/0334r0.IEEE Std. 802.11 TGad, Mar. 2009.

Hsi-Lu Chao (M'09) received the B.S. degree in electronics engineering from Feng Chia University, Taichung, Taiwan, in 1992, the M.S. degree in electrical engineering from the University of Southern California, Los Angeles, in 1996, and the Ph.D. degree in electrical engineering from the National Taiwan University, Taipei, Taiwan, in 2004.

Since August 2004, she has been an Assistant Professor with the Department of Computer and Information Science, National Chiao Tung University, Hsinchu, Taiwan. Her research interests include cognitive radio networks, millimeter-wave personal area networks, Fourth-Generation networks, cooperative communications, and heterogeneous wireless networks.

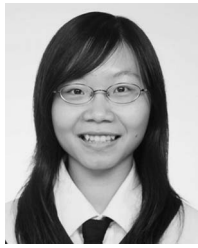

Ming-Pei Hsu received the B.S. and M.S. degrees from the National Chiao Tung University, Hsinchu, Taiwan, in 2008 and 2010, respectively.

She is currently a Software Engineer with the Software Eng'g Div I, Wireless Communications Business Unit, MediaTek Inc., Taipei, Taiwan.